Tomography of the Mojavian Lithosphere Viscosity from Space Geodetic data of the Landers and Hector Mine Earthquakes

Sylvain Barbot[1,2] and Yuri Fialko[2], [1]California Institute of Technology, [2]Scripps Institution of Oceanography

SCEC an NSF + USGS center
IGPP
Caltech

Motivations

We investigate the transient deformation following the 1992 Mw7.3 Landers and the 1999 Mw7.1 Hector Mine earthquakes (Mojave desert, Southern California) using a combination of GPS and InSAR for an interval spanning 1992 to 2010. We test the possible mechanisms of postseismic relaxation using physically-based time-dependent models of deformation driven by coseismic stress changes. Considered mechanisms include viscoelastic flow in the lower crust and upper mantle, afterslip governed by a rate-dependent friction, and poroelastic rebound. We find that both afterslip and viscoelastic relaxation models can explain the horizontal post-Landers GPS data equally well. Afterslip however gives rise to vertical displacements of opposite polarity to the ones measured by GPS. A viscoelastic model marked by a strong (high viscosity) lower crust and weak (low viscosity) upper mantle transitioning at a depth of 40km gives rise to large wavelength LOS deformation in the near field which is not observed in the InSAR data. Poroelasticity models are consistent with wavelength of InSAR LOS displacements and campaign GPS vertical data, but cannot explain the azimuth and amplitude of horizontal displacements. None of these simple models can explain all the available geodetic measurements simultaneously and a more complex explanation is required, involving either multiple mechanisms or more spatial variations in material properties.

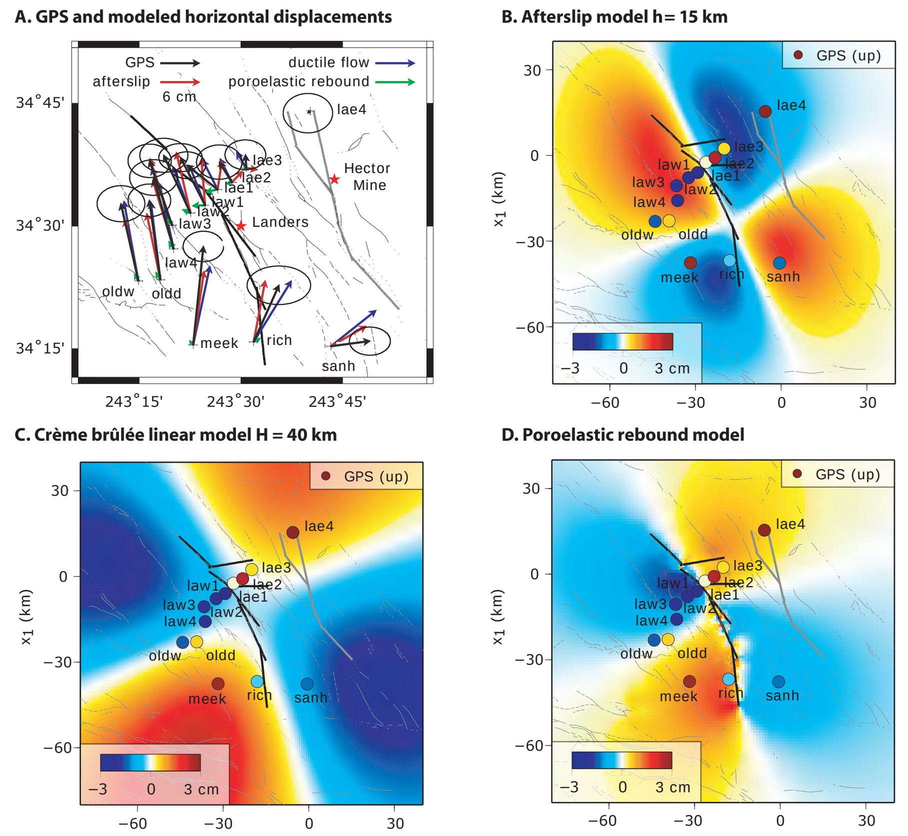

A. GPS and modeled horizontal displacements
B. Afterslip model h= 15 km
C. Crème brûlée linear model H = 40 km
D. Poroelastic rebound model

Jelly Sandwich vs Schizosphere end-member models: A strong trade-off

Freed et al (2007) showed that a scenario of afterslip after the 1992 and 1999 Mojave earthquakes led to significant misfit at most GPS stations, but afterslip as a single driver of the postseismic transient is also ruled out by the anti-correlation of predicted and observed vertical displacements. The question of the possible contribution of afterslip in a predominantly viscous-flow-driven transient remained. We consider a simple scenario with only ductile flow in the asthenosphere below a depth H. A deeper transition to viscous flow implies a dramatic amplitude decrease of near-field and far-field displacements. For comparison, we evaluate the postseismic response to the same fictitious event considering a scenario of rate-strengthening creep in a plastic zone from the bottom of the seismogenic zone h=15km transitioning to distributed viscous flow at depth H, the so-called schizosphere model. We assume similar relaxation time scales for creep and viscous flow. The patterns of horizontal displacements are virtually indistinguishable from the ones predicted by viscoelastic flow alone. The vertical displacements however are quite different, with a near-field vertical displacement dominated by afterslip in the far-field one dominated by the viscous flow. In principle the mechanisms may be discriminated with the near-field data.

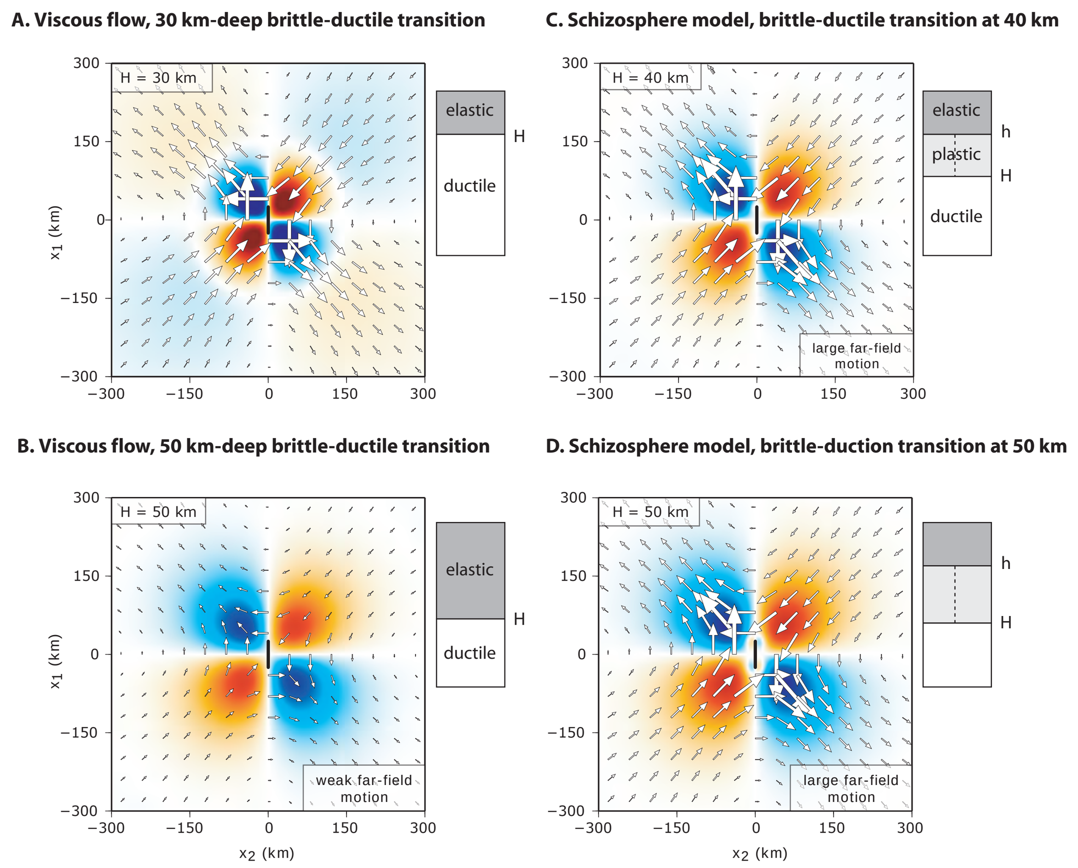

A. Viscous flow, 30 km-deep brittle-ductile transition
C. Schizosphere model, brittle-ductile transition at 40 km
B. Viscous flow, 50 km-deep brittle-ductile transition
D. Schizosphere model, brittle-duction transition at 50 km

Jelly Sandwich vs Schizosphere end member models

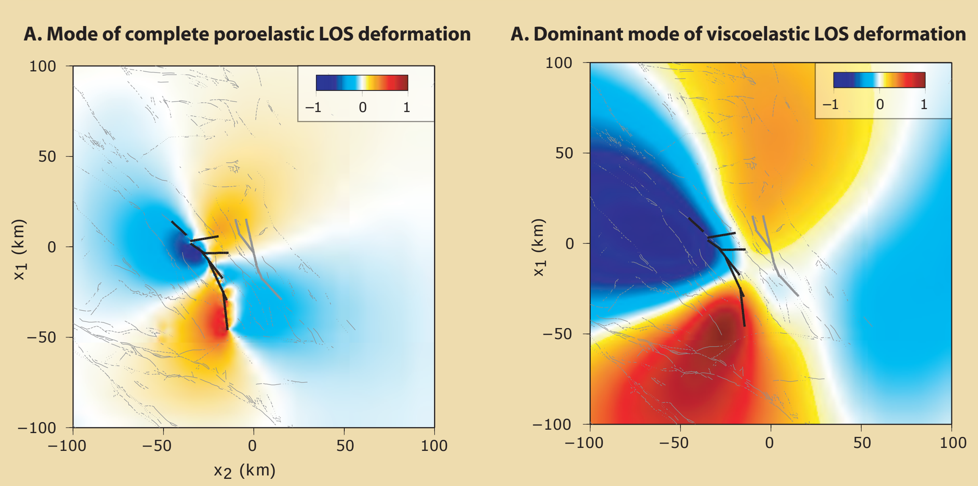

A. Mode of complete poroelastic LOS deformation
A. Dominant mode of viscoelastic LOS deformation

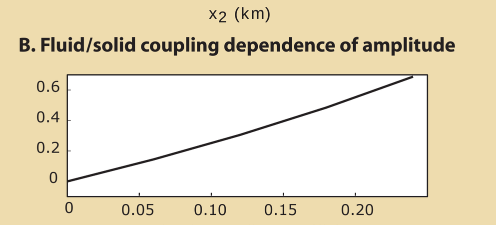

B. Fluid/solid coupling dependence of amplitude

Inversion of the inelastic properties of the subsurface has often relied on minimizing a misfit function by a numerically costly exploration of a parameter space, which is kept small due to computational limitations. The method of data reduction by exploration of a model space is justified because no single deformation mechanism is self similar, even with a linear rheology, leading to time series of surface displacement that are not separable in space and time. We challenge this idea by showing that time series of viscoelastic or afterslip surface deformation are dominated by a time-space separable component. A similar result holds for afterslip assuming steady creep. For these mechanisms, the second mode of deformation is negligible compared with noise in InSAR due to atmospheric delays and uncertainties in forward models of deformation caused by approximations in the numerical quadrature. It follows that for inversion purposes one may consider that forward models of afterslip and viscoelastic relaxation are separable in space and time to a reasonable degree of approximation. For complete poroelastic rebounds, the spatial distribution of deformation is identical for all values of poroelastic coupling, and only the amplitude of the deformation varies.

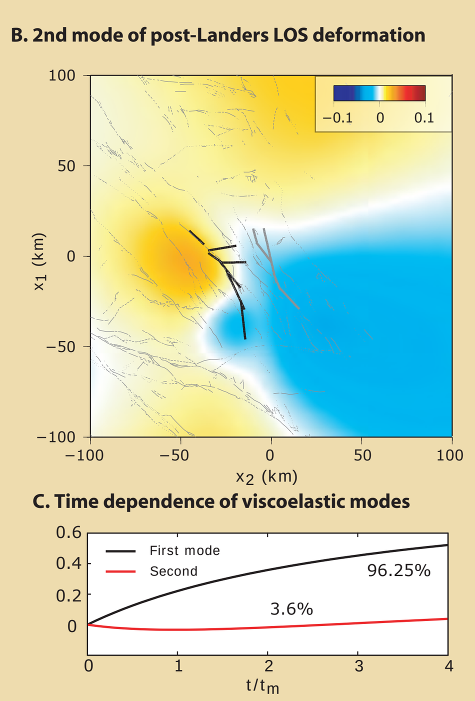

B. 2nd mode of post-Landers LOS deformation
C. Time dependence of viscoelastic modes

Resolution on inelastic properties

For the 1992-1999 time interval, InSAR and campaign GPS offer similar resolution, with a clear capacity to constrain the fluidity of the most shallow ductile stratum and that of the deepest substrate. At intermediate depths however, the resolution on fluidity is quite poor, with values decaying from R=50% to R=5%. The low resolution of post-Landers InSAR data explains the numerous tradeoffs between possible models. For the post-Hector Mine epochs the InSAR Green function includes elements from the viscous relaxation of the Landers and Hector Mine ruptures and one important effect is to significantly improve the resolution on the second-most shallow layer. In the post-Hector Mine epoch the GPS Green function includes more numerous stations with an increase in spatial coverage that leads to an improve resolution of the fluidity structure at intermediate depths. We performed the same analysis including poroelasticity in the design matrix. We found that the contribution of poroelasticity for both the Landers and Hector Mine periods is well constrained, with a resolution of 99.9% without important effects on the fluidity resolution except for the two deepest thin ductile layers.

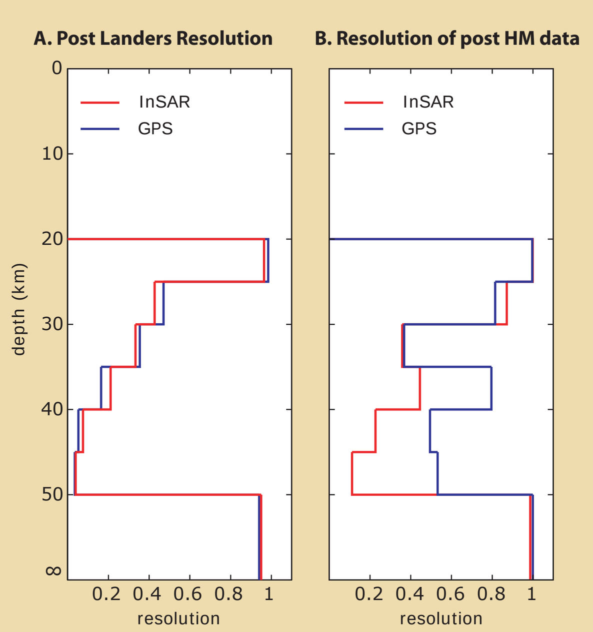

A. Post Landers Resolution
B. Resolution of post HM data

Analysis of post-Landers Insar data

We exploration the possible models that can explain the post-Landers InSAR data alone, we find that some afterslip may take place on the downward extension of the coseismic rupture, in combination to viscoelastic flow at greater depths. A more plausible mechanism, however, is viscoelastic relaxation in the lower crust and upper mantle, with no or little contribution from fault creep in the time interval considered. All model considered (either viscoelastic or schizosphere models) give rise to better variance reduction if a poroelastic rebound is also accounted for. Inference of a viscosity profile for all scenarios differ principally by the required viscosity of the lower crust, with a lower-crust viscosity about one order of magnitude higher in the model including poroelastic rebound. One feature that persists in all inversions is the geometry of the viscous flow. All models require flows in the lower crust and in the upper mantle separated by a competent layer below the Moho. The presence of a mantle lid between the lower-crustal and the deep upper mantle flows is the preferred model but models that assume more gradual variations in viscosity as a function of depth still give rise to reasonable variance reduction of the geodetic data.

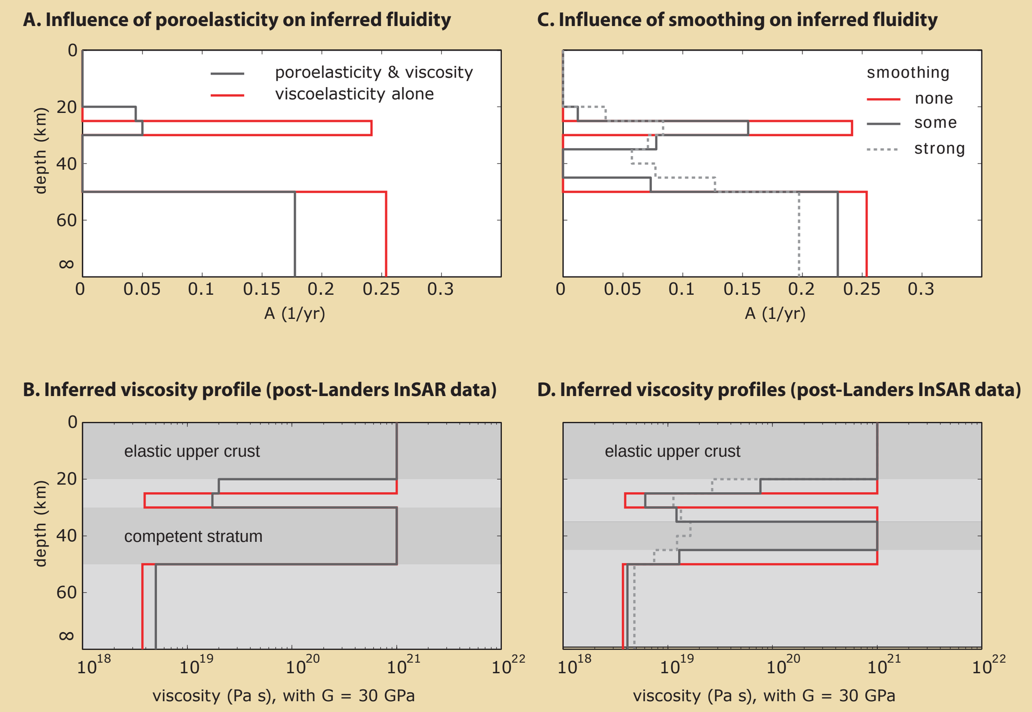

A. Influence of poroelasticity on inferred fluidity
C. Influence of smoothing on inferred fluidity
B. Inferred viscosity profile (post-Landers InSAR data)
D. Inferred viscosity profiles (post-Landers InSAR data)

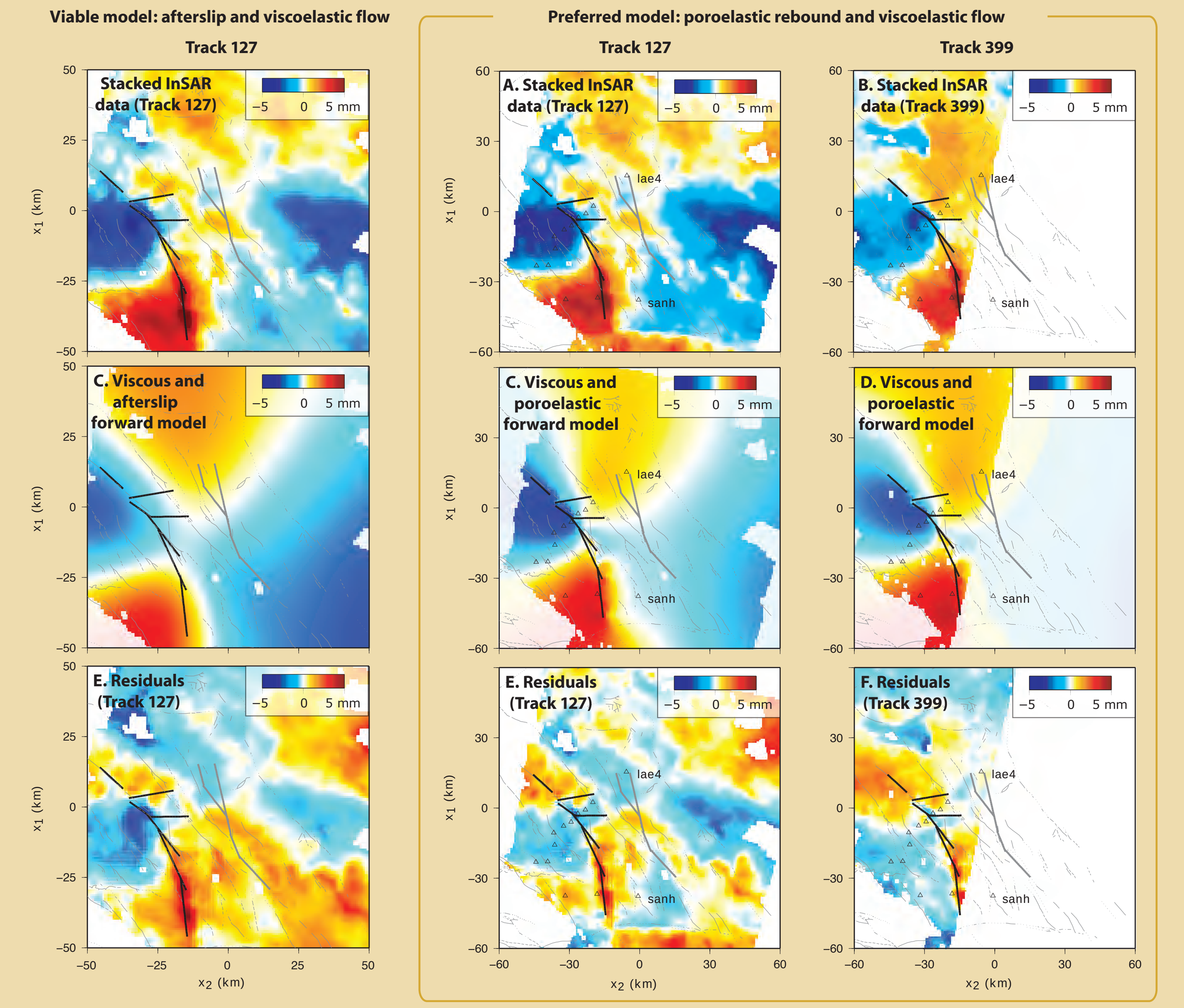

Viable model: afterslip and viscoelastic flow
Preferred model: poroelastic rebound and viscoelastic flow

Analysis of post-Landers and post-Hector Mine Insar and GPS data: Evidence for Jelly-Sandwich lithosphere & poroelastic rebound

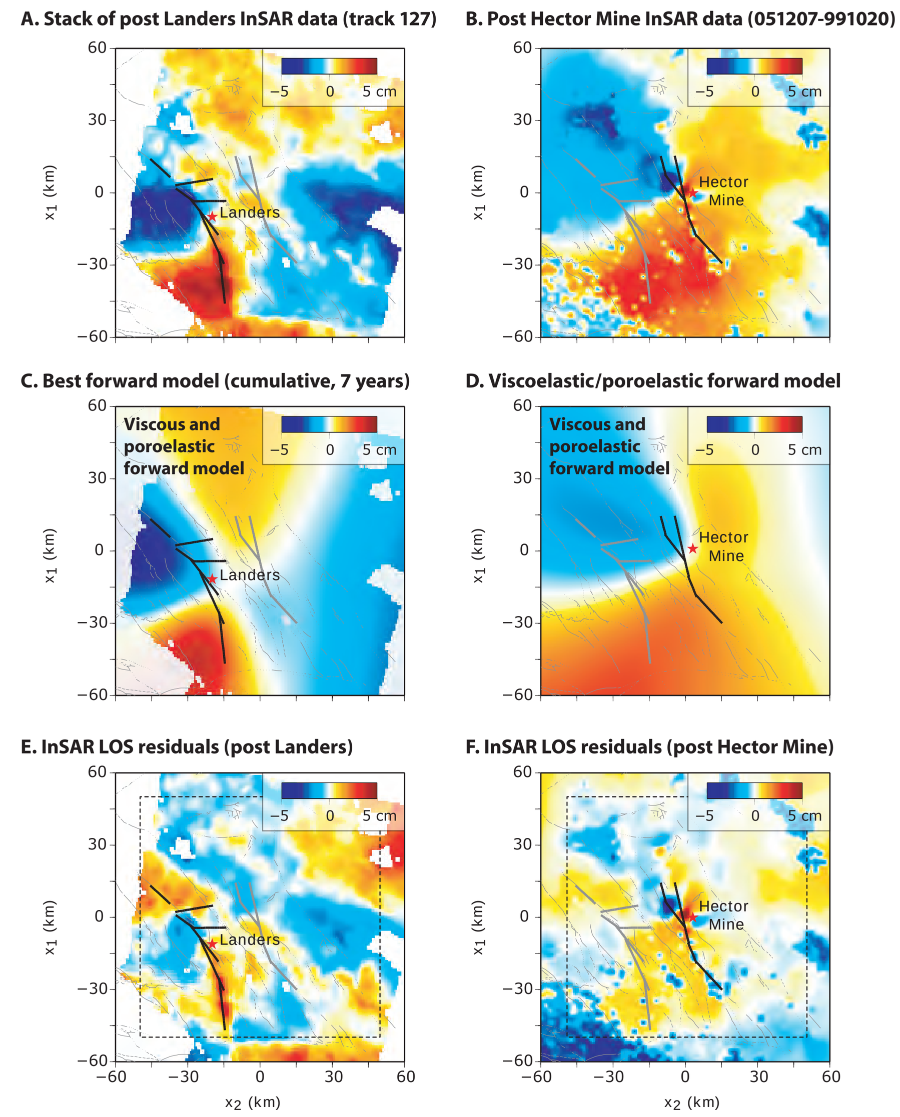

A. Stack of post Landers InSAR data (track 127)
B. Post Hector Mine InSAR data (051207-991020)
C. Best forward model (cumulative, 7 years)
D. Viscoelastic/poroelastic forward model
E. InSAR LOS residuals (post Landers)
F. InSAR LOS residuals (post Hector Mine)

The best-fitting model implies a combination of poroelastic rebound in the entire lithosphere accompanied with viscoelastic flow in the lower and the upper mantle. Yet, other models that give rise to somewhat less variance reduction of the geodetic data may still be valid explanation of the postseismic relaxation. In particular, another viable model implies deep afterslip on a down-dip extension of the rupture fault that transitions to viscoelastic flow at greater depth, with a wide-spread poroelastic rebound in the entire lithosphere. If the assumption of the presence of sharp variations in viscosity is verified, all models imply the presence of a mantle lid below the Moho, corresponding to a jelly-sandwich strength model of the lithosphere. The effect of other mechanisms on the inferred strength of the lithosphere is to increase the lower-crustal viscosity compared to models that imply viscoelastic flow alone.

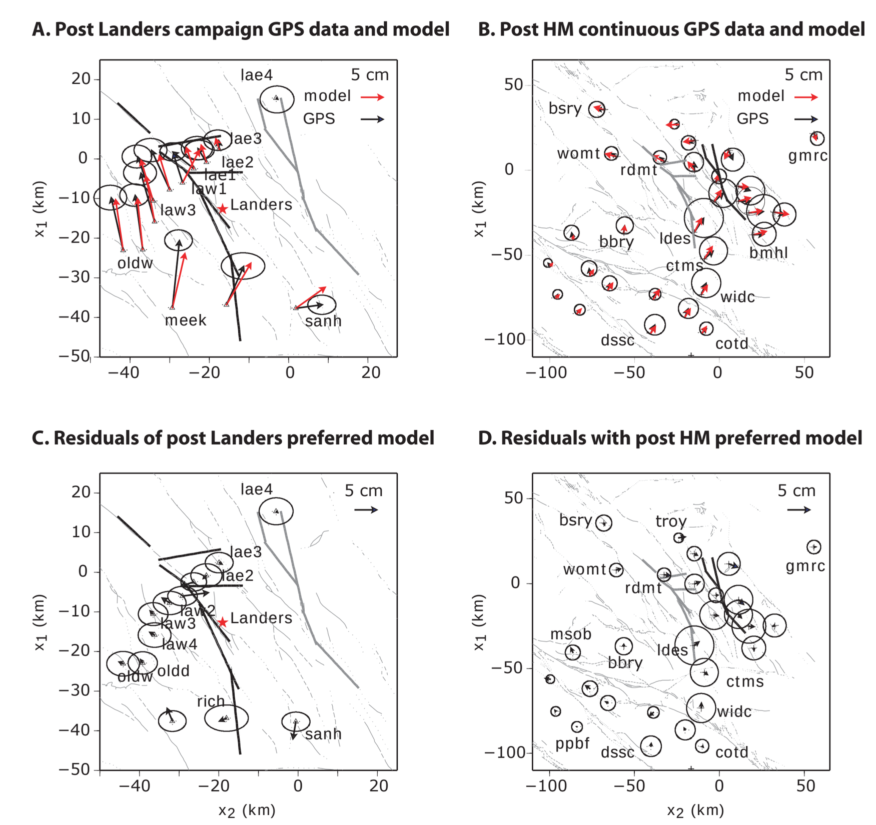

A. Post Landers campaign GPS data and model
B. Post HM continuous GPS data and model
C. Residuals of post Landers preferred model
D. Residuals with post HM preferred model

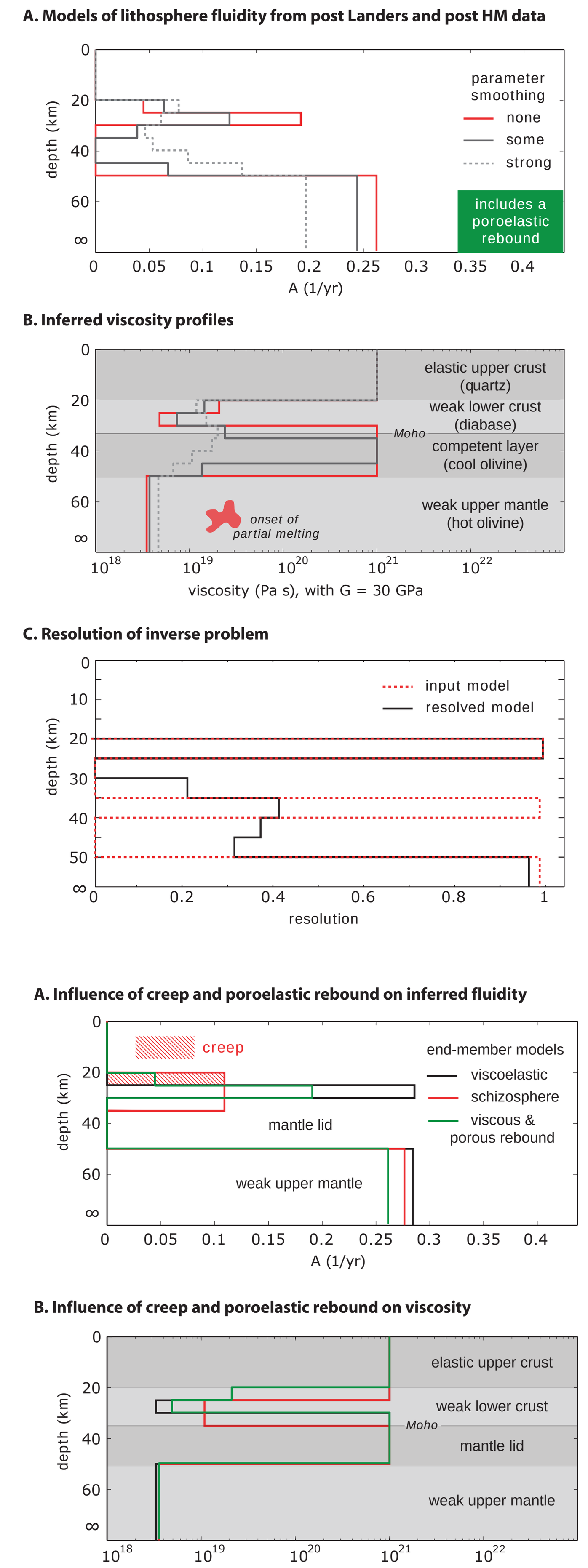

A. Models of lithosphere fluidity from post Landers and post HM data
B. Inferred viscosity profiles
C. Resolution of inverse problem
A. Influence of creep and poroelastic rebound on inferred fluidity
B. Influence of creep and poroelastic rebound on viscosity

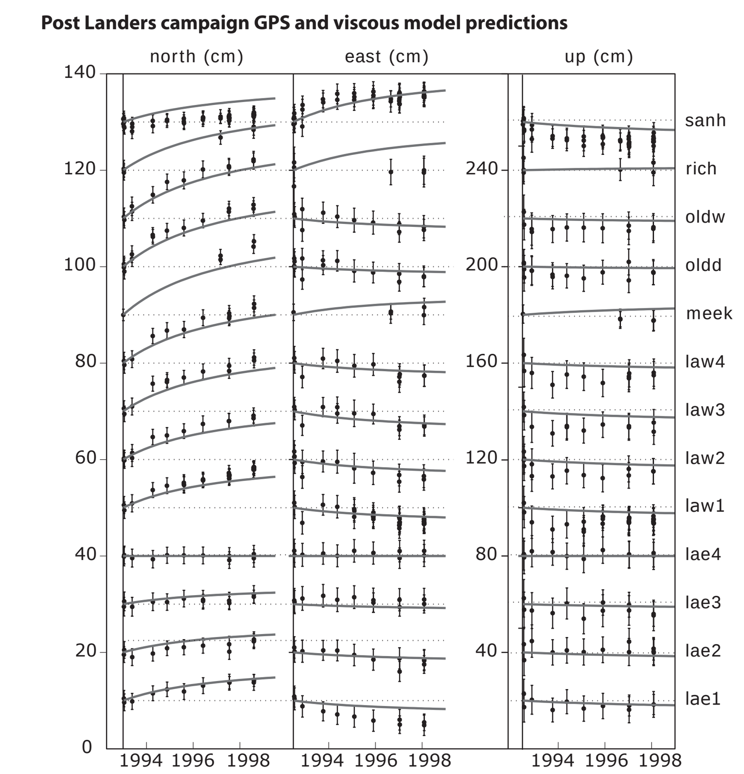

Post Landers campaign GPS and viscous model predictions

We compare the time series of continuous GPS data in the period following the 1999 Hector Mine earthquake. sThe variance reduction of the cumulative post-Hector Mine GPS displacements are 81.5%. Similarly, about 20% of all stations show some misfit between forward models time series and observed displacements. For those stations that do not exhibit misfit at the tail of the time series, the model explain the displacement in the entire time interval successfully. It is quite remarkable that the viscoelastic model, with only seven degrees of freedom and only two low-viscosity layers can explain so various data sets including spatial variations of LOS displacements, campaign GPS and continuous GPS data.

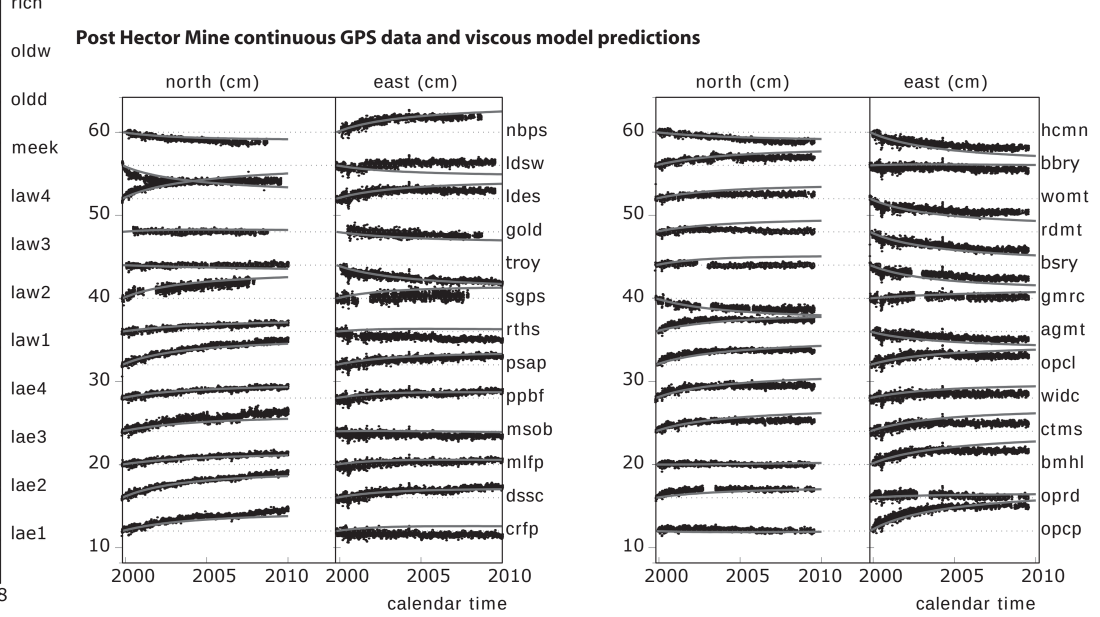

Post Hector Mine continuous GPS data and viscous model predictions

Geological interpretation & Concluding remarks

Our results imply relaxation in a shallow ductile layer, between 25 and 30km depth, coincident with the Moho discontinuity. The lower-crustal flow is separated from the mantle flow below 50km by a 20km-thick competent layer at intermediate depths. Assuming a constant shear modulus of 30GPa, the model implies similar viscosities in the lower and mantle of 3.5E18 Pa s. Given the resolution of the inverse problem, the inference of a weak lower crust is robust, but we cannot rule out more gradual variations of viscosity as these models still offer reasonable fit to the geodetic data sets. A contribution of afterslip may bias our preferred viscoelastic model towards a lower viscosity but our inference of a viscosity profile characterized by two low-viscosity horizons in the lower crust and upper mantle is little affected by the presence of shallow afterslip.

Using InSAR and GPS data from the post-Landers and post-Hector Mine epochs, we constrained lateral variations in viscosity below the Mojave Desert. Data require a low-viscosity anomaly to the South-West of the Landers rupture, towards the San Andreas Fault. Tomography of the viscous structure indicates a thickening of the shallowest ductile stratum near the San Gabriel segment of the San Andreas fault coincidental with the deepening of the Moho at this location. Our results indicate that the Moho might mark not only a strong elastic boundary, but might also delineate a strong viscosity contrast between mantle and crustal material. This view is consistent with constraints of the continental lithospheric strength from laboratory experiments.

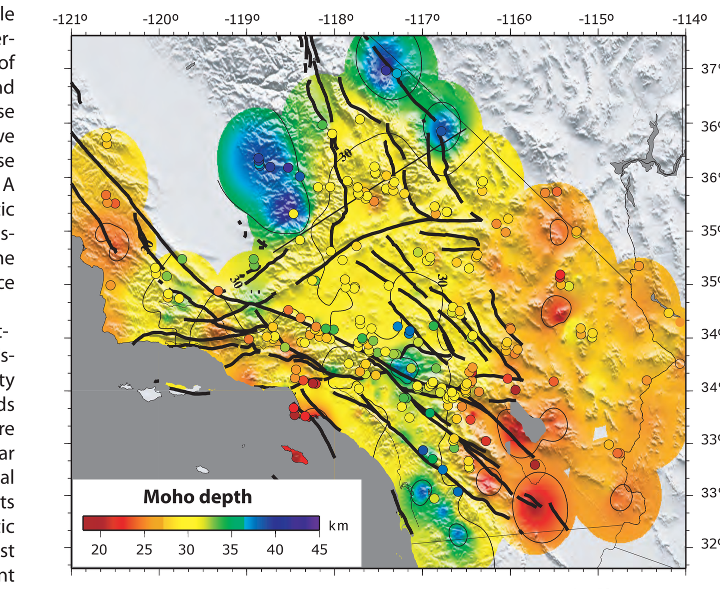

Yan & Clayton, 2007

Regional S-wave receiver function analysis resolve a relatively sharp asthenosphere-lithosphere boundary at ~65km with sharpness <20km [Li et al., 07]. Regional P-wave receiver function analysis resolves a sharp Moho beneath the region at ~30km [Yan & Clayton, 07]. Petrogenetic data on mantle xenoliths that were entrained in late Cenozoic volcanic rocks of the region, further constrained by surface heat flow data, resolve mantle lithosphere peridotites between ~30 and ~50km that are considerably cooler than peridotite xenoliths entrained from asthenosphere depths [Luffi et al, 09]. Crustal basement rocks typical of the central Mojave region are exposed to lower crustal levels around the periphery of the Mojave Desert as a series of core complexes [Saleeby et al., 07]. These exposures show that the crust is quartz bearing and hydrous to 30-35 km depths, and thereby capable of fluid behavior under lower crustal conditions.

The presence of a weak lower crust is supported by the presence of rock with low- to intermediate-temperature activation creep, such a quartzites, granites or diabase and diorite. Mantle rocks, such as olivine, are characterized by a higher-temperature activation creep so that there is a strong decrease in viscosity with depth. The temperature dependence of viscosity leads to the division of the upper mantle into a competent (high viscosity) upper layer below the Moho and a weaker substrate at depths greater than ~50km. A number of geologic and geophysical constraints when considered together resolve a lithospheric structure beneath the central Mojave region that is consistent with the fluidity and inferred viscosity profiles.

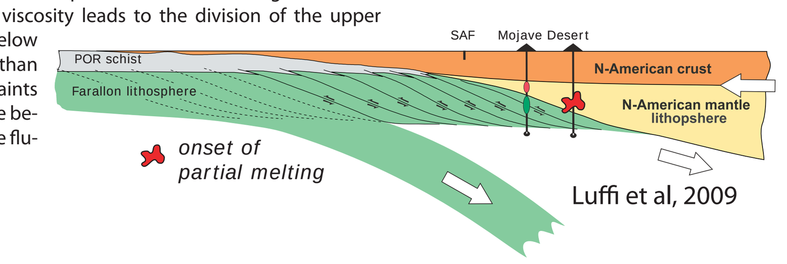

Luffi et al, 2009

schematic yield envelope

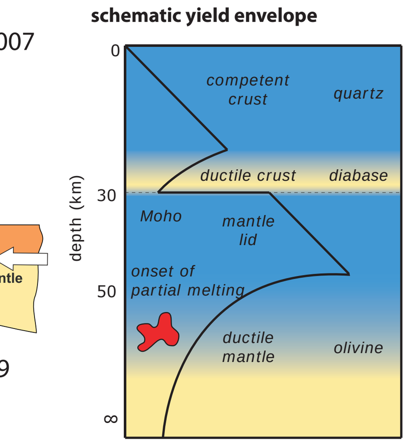

Tomography of lateral variations of viscosity

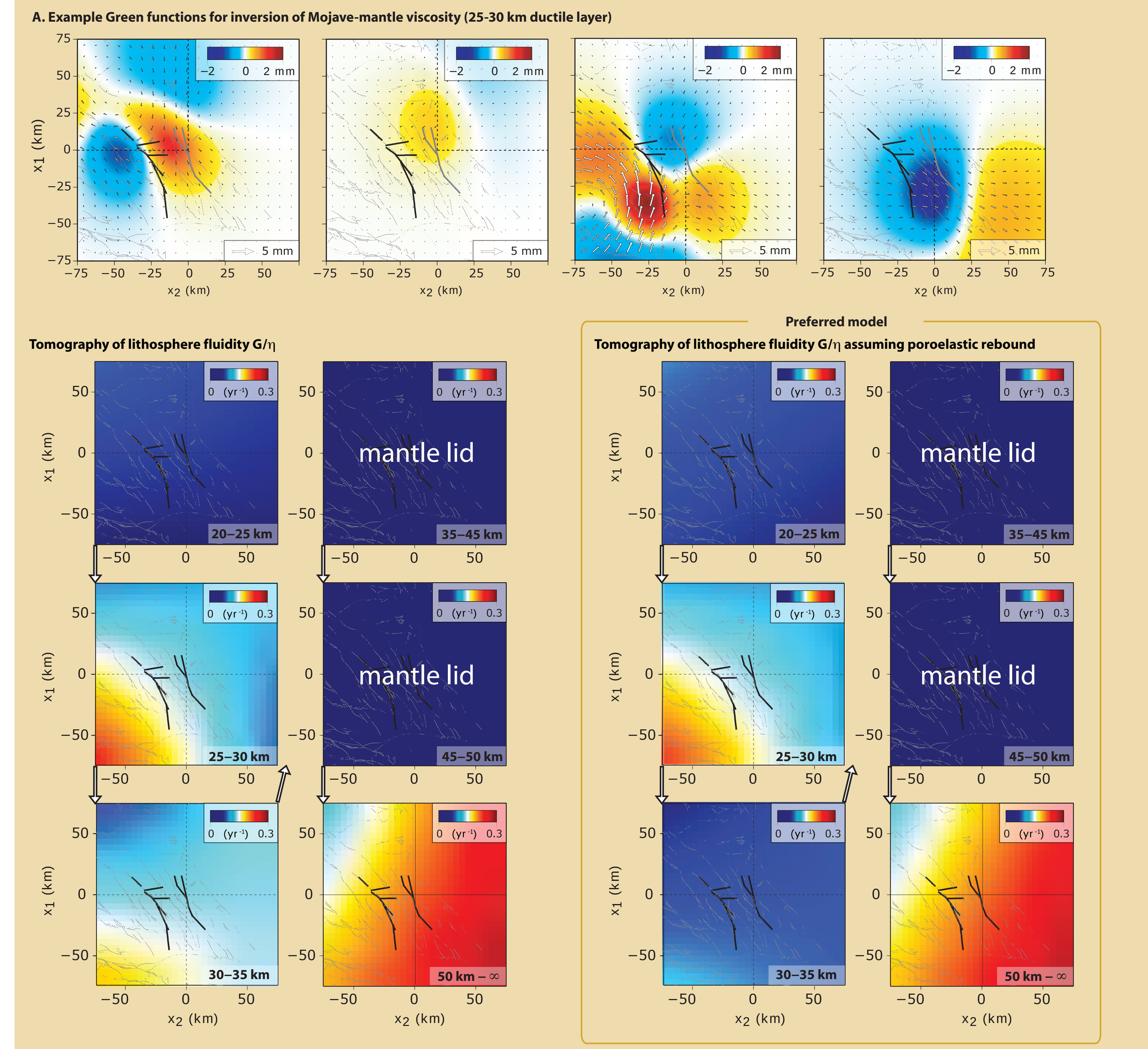

A. Example Green functions for inversion of Mojave-mantle viscosity (25-30 km ductile layer)
Tomography of lithosphere fluidity G/η
Preferred model
Tomography of lithosphere fluidity G/η assuming poroelastic rebound

References

L. Bruhat, Barbot S. and Avouac J.-P., "Contributions of Afterslip and Viscoelastic Flow Following the 2004 Parkfield Earthquake", Geophysical Research Letters, submitted, 2010

S. Barbot and Y. Fialko, “Tomography of the Mojavian Lithosphere Viscosity from Space Geodetic data of the Landers and Hector Mine Earthquakes”, Geophys. J. Int., submitted, 2010

S. Barbot and Fialko Y., "A Unified Continuum Representation of Postseismic Relaxation Mechanisms: Semi-Analytic Models of Afterslip, Poroelastic Rebound and Viscoelastic Flow", Geophys. J. Int., v. 182, Issue 3, p. 1124-1140, 2010

S. Barbot and Fialko Y., "Fourier-Domain Green Function for an Elastic Semi-Infinite Solid under Gravity, with Applications to Earthquake and Volcano Deformation", Geophys. J. Int., in press 2010

S. Barbot, Fialko Y., Sandwell D., "Three-dimensional models of elasto-static deformation in heterogeneous media, with application to the East California Shear Zone", Geophys. J. Int., v. 179, no. 1, p. 500-520, 2009

E. S. Cochran, Li Y.-G., Shearer P., Barbot S., Fialko Y., Vidale J. E., "Seismic and Geodetic Evidence For Extensive, Long-Lived Fault Damage Zones", Geology, v. 37, no. 4, p. 315-318, 2009

S. Barbot, Fialko Y., Bock Y., "Postseismic Deformation due to the Mw6.0 2004 Parkfield Earthquake: Stress-Driven Creep on a Fault with Spatially Variable Rate-and-State Friction Parameters", J. Geophys. Res., vol. 114, B07405, 2009